Organic & Biomolecular Chemistry

ROYAL SOCIETY OF CHEMISTRY

COMMUNICATION

View Article Online
View Journal | View Issue

Cite this: *Org. Biomol. Chem.*, 2021, **19**, 6995

Received 7th May 2021,
Accepted 2nd August 2021

DOI: 10.1039/d1ob00903f

rsc.li/obc

Scalable ^{18}F processing conditions for copper-mediated radiofluorination chemistry facilitate DoE optimization studies and afford an improved synthesis of [^{18}F]olaparib†

Gregory D. Bowden, [a] Nantanat Chailanggar,[a] Bernd J. Pichler[a,b,c] and Andreas Maurer *[a,b]

A convenient and scalable base-free method for processing [^{18}F] fluoride as [^{18}F]TBAF is reported and applied to copper-mediated radiofluorination radiosyntheses. A central feature of this method is that a single production of [^{18}F]TBAF can be divided into small aliquots that can be used to perform multiple small-scale reactions in DoE optimization studies. The results of these studies can then be reliably translated to full batch tracer productions using automated synthesizers. The processing method was applied to the DoE optimization of [^{18}F]olaparib, affording the tracer in high radiochemical yields *via* both manual (%RCY = 78 ± 6%, *n* = 4 (CMRF step only)) and automated (up to 80% (%RCY); 41% activity yield (%AY)) radiosynthesis procedures.

As the use of positron emission tomography (PET) as a molecular imaging tool continues to grow, so will the demand for novel clinically relevant PET tracers. The development of new automatable radiochemical methodologies, particularly for ^{18}F radiochemistry, has become an important area of research to meet this demand. The copper-mediated radiofluorination (CMRF) family of aromatic radiofluorinations is a recent example of a "next-generation" radiochemical methodology that has become a highly relevant tool for radiolabeling aromatic compounds with ^{18}F.[1–3] The methodology's broad scope and operational simplicity have meant that radiopharmacy research groups have readily adopted it as a convenient method for rapidly developing novel tracers for preclinical evaluation.[4] As these tracers become more utilized by preclinical and clinical imaging scientists, radiopharmacists must adapt "next-gen" radiolabeling methods, like CMRF chemistry, to meet the expanding tracer production demands.[5] Radiosynthesis optimization is an essential part of this process. A well-optimized radiosynthesis (in terms of both chemistry and purification) is more reliable and ensures maximal activity yields, thus making radiopharmaceutical production more efficient in light of the continuously increasing demand for PET radiotracers. Additionally, carefully optimizing radiosyntheses can help minimize the use of potentially toxic reagents, precursors, solvents, or catalysts. From a GMP perspective, simplified tracer production, purification, and expedited quality control procedures can make it easier for radiopharmacies to meet the regulatory requirements regarding solvent and impurity content.

"Design of Experiments" (DoE) is a statistical toolset that aims to provide a detailed model of processes' performance with respect to multiple experimental variables (factors) while minimizing the number of optimization experiments.[6] We have previously reported that using a DoE approach expedites the radiosynthesis optimization process in terms of cost and time and can extract practically useful information in the form of response surface models (RSMs).[7] This information can then be used to develop more efficient radiosynthesis protocols with more limited use of harmful substances. This work laid the basis for a DoE based tracer development pipeline that increases the rate at which radiopharmacists can establish, optimize, automate, and deliver CMRF-based tracer productions for preclinical study.

This initial work focused on optimizing reaction conditions and assumed little influence from the ^{18}F processing method. However, the processing of [^{18}F]fluoride is an essential step in any ^{18}F-radiosynthesis, and it can indeed have a significant influence on the final yield. The purpose of ^{18}F processing is to dehydrate the [^{18}F]fluoride ion and provide an appropriate counter ion to maximize the nucleophilicity of the [^{18}F]fluoride ion before its reaction with a substrate. For practical reasons, the DoE studies mentioned above were performed using small aliquots (80 μl) of a [^{18}F]KF solution eluted from a single QMA (quaternary methylammonium resin) cartridge with a solution of potassium triflate and potassium carbonate in water (Fig. 1,

[a]*Werner Siemens Imaging Center, Department of Preclinical Imaging and Radiopharmacy, Eberhard Karls University, Tübingen, Germany. E-mail: andreas.maurer@med.uni-tuebingen.de*
[b]*Cluster of Excellence iFIT (EXC 2180) "Image-Guided and Functionally Instructed Tumor Therapies", Eberhard Karls University, Tübingen, Germany*
[c]*German Cancer Research Center, German Cancer Consortium DKTK, Partner Site Tubingen, D-72076 Tübingen, Germany*

†Electronic supplementary information (ESI) available. See DOI: 10.1039/d1ob00903f

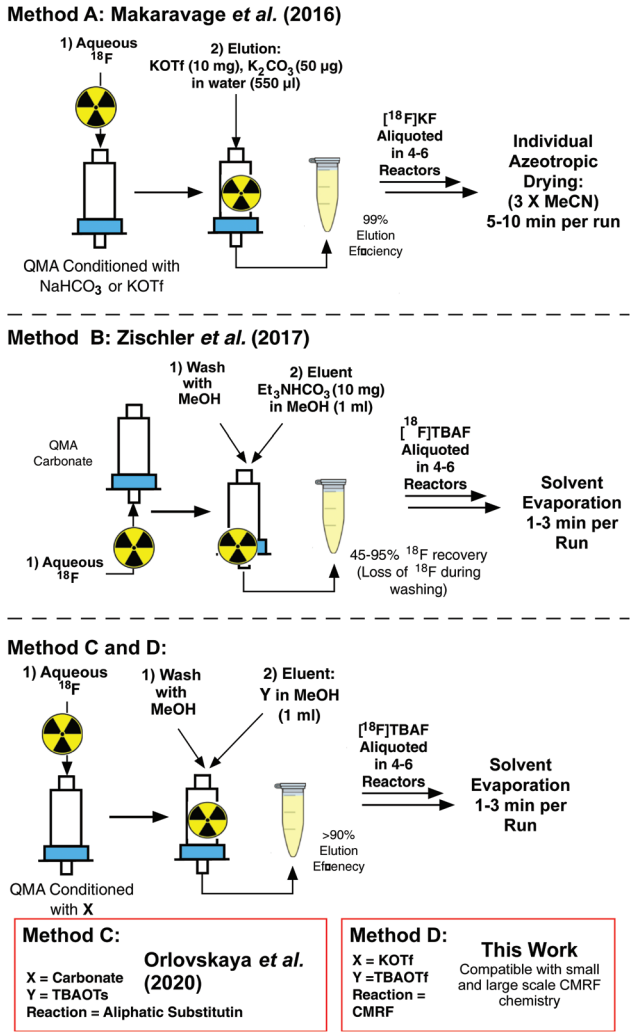

Fig. 1 Previous (methods A-C) and current (method D) work into the development of CMRF specific ^{18}F processing methods.

Method A), as initially described by Makaravage *et al.*[3] These aliquots of [^{18}F]KF solution were then transferred into 5–6 reaction vessels and were individually azeotropically dried with three additions of acetonitrile (1.5 ml) by the standard method. While laborious and time-consuming, this method ensured a relatively even distribution of [^{18}F]fluoride and QMA eluent salts between the reaction vessels, reducing experimental variability in the DoE studies. It also allowed multiple experiments to be conducted from one delivery of cyclotron produced [^{18}F]fluoride, making the use of multi-experiment DoE studies a practical possibility. However, in many instances, the results obtained from these DoE studies did not scale up when performed with "batch" quantities of QMA eluents. The deleterious effects of larger amounts of carbonate bases and phase transfer catalysts (PTCs) present in QMA eluent solutions on CMRF reactions have been well documented.[8–11]

To further our work in establishing a rapid tracer development and radiosynthesis optimization pipeline around the DoE approach, we required an ^{18}F processing method that met the following requirements: (1) The procedure needed to be operationally simple, fast, scalable, and automatable using standard radiosynthesis modules. (2) Given our desire to carefully study the effect of various reaction components (*e.g.*, pyridine load, not discussed in this work) on CMRF reactions' performance, the QMA eluent should minimize any components that may affect or interact with either the copper-mediator or the precursor. We thus wanted to avoid the use of eluents that included the precursor, catalyst, or pyridinium salts (as successfully employed by Zhang *et al.* and Antuganov *et al.*)[12,13] (3) The method should eliminate the use of strongly basic anions (*e.g.*, carbonates) and cryptand PTCs from the QMA preconditioning and eluent solutions to ensure true scalability from "aliquoted" DoE reaction studies to full "batch" radiosyntheses.

Several groups have investigated alternative QMA cartridge eluents that are less basic and better suited to CMRF chemistry than the classic combination of potassium carbonate and Kryptofix® 2.2.2 (K_{222}).[10–18] Tetraalkylammonium salts and their alcohol adducts have long been studied as facilitators of traditional fluorination reactions.[19–22] Their use has since been adapted for various radiofluorination strategies. One of the more widely adopted methods has been the alcohol-enhanced CMRF developed by Zischler *et al.* (Fig. 1, Method B), whereby the [^{18}F]fluoride was efficiently eluted from the QMA using tetraethylammonium bicarbonate (TEAB) in an alcoholic solvent.[16] This method could provide processed ^{18}F from the QMA cartridge with high elution efficiency and could be used to synthesize several radiotracers in good to excellent radiochemical yields. However, the technique suffered a significant drawback: the aqueous ^{18}F needed to be loaded onto the cartridge in the reverse direction to ensure maximal elution efficiency. This "back-flushing" procedure adds operational complexity and increases the probability of introducing radiochemical impurities from the irradiated cyclotron target water into the reactor vessel.

Orlovskaya *et al.* showed that tetrabutylammonium tosylate (TBAOTs) in an alcoholic solvent was able to efficiently elute [^{18}F]fluoride from a QMA-bicarbonate cartridge (QMA-HCO_3, QMA cartridge with bicarbonate counter ion) (Fig. 1, Method C).[23] TBAOTs was also found to be suitable as a stable and inert PTC for traditional S_N2 radiofluorinations. The authors were able to show that TBAOTs in ethanol could elute ^{18}F from a QMA-HCO_3 cartridge with a high elution efficiency (>90%) without needing to load the ^{18}F onto the QMA cartridge in the reverse direction. The authors later reported the CMRF compatibility of similar ^{18}F processing chemistry (using the "back-flushing" protocol discussed above) when applied to the CMRF synthesis of 6-L-[^{18}F]FDOPA.[24] Inspired by this fast and operationally simple approach, we aimed to develop an ^{18}F processing method that entirely eliminates the presence of carbonate base from a CMRF reaction mixture by preconditioning the QMA cartridge with an organic sulfonate anion (Fig. 1, Method D).

A series of experiments were performed to evaluate and compare different ^{18}F processing protocols, each featuring an ^{18}F processing step, followed by either azeotropic drying or solvent evaporation under a stream of argon (Table 1). Each

Table 1 Experiments to test both the ^{18}F elution efficiency and the QMA eluent mixture's effect on CMRF reaction performance of various ^{18}F processing methods

Entry (reference)	Percon. salt	Loading direction	Eluent PTC salt	Base	Eluting solvent	Vol (µl)	MeOH Wash (1 ml)	% ^{18}F recovery	Azeotropic drying (3X MeCN)	%RCY [^{18}F]1[a]
1	$NaHCO_3$ (1 M)	Forward	K_{222} (6.4 mg)	$K_2CO_3/K_2C_2O_4$	MeCH : H_2O (4 : 1)	1000	No	33	Yes	3
2	$NaHCO_3$ (1 M)	Forward	K_{222} (9.5 mg)	K_2CO_3 (1.7 mg)	MeCH : H_2O (4%)	2000	No	97	Yes	ND
3	$NaHCO_3$ (1 M)	Forward	KOTf (10 mg)	K_2CO_3 (50 µg)	H_2O	550	No	94	Yes	8
4	KOTf	Forward	KOTf (10 mg)	K_2CO_3 (50 µg)	H_2O	550	No	98	Yes	13
5	KOTf	Forward	TBAOTf (10 mg)	Cs_2CO_3 (50 µg)	H_2O	550	No	99	Yes	33
6	KOTf	Forward	TBAOTf (5 mg)	—	H_2O	550	No	96	Yes	32
7	KOTf	Forward	TBAOTf (10 mg)	—	H_2O	550	No	96	Yes	24
8	KOTf	Reverse	TBAOTf (5 mg)	—	MeOH	1000	Yes	44	MeOH Evap	73
9	KOTf	Reverse	TBAOTf (10 mg)	—	MeOH	1000	Yes	45	MeOH Evap	71
10	KOTf	Forward	TBAOTf (5 mg)	—	MeCN	1000	Yes	0	NR	NR
11	KOTf	Forward	TBAOTf (10 mg)	—	MeCN	1000	Yes	0	NR	NR
12	KOTf	Forward	TBAOTf (5 mg)	—	EtOH	1000	Yes	81	EtOH Evap	55
13	KOTf	Forward	TBAOTf (10 mg)	—	EtOH	1000	Yes	79	EtOH Evap	62
14	KOTf	Forward	TBAOTf (5 mg)	—	MeOH	1000	Yes	92 ± 1.4	MeOH Evap	67 ± 3.1[b]
15	KOTf	Forward	TBAOTf (10 mg)	—	MeOH	1000	Yes	93 ± 2.2	MeOH Evap	64 ± 1.5[b]
16	KOTf	Forward	TBAOTf (1 mg)	—	MeOH	1000	Yes	58 ± 3.0	MeOH Evap	40 ± 1.4[b]
17	KOTf	Forward	TBAOTf (10 mg)	—	MeOH	1000	No	95 ± 0.4	MeOH Evap	72 ± 8.9[b]

[a] Radiochemical yields are calculated directly from radio TLC; ND, No producted detected; NR, No result as the experiment was not performed. [b] Experiments performed in triplicate (mean ± standard deviation).

Scheme 1 Model reaction to test ^{18}F processing parameters.

run was performed using a batch ^{18}F elution from a single QMA cartridge. An unoptimized model CMRF reaction using 4-biphenylboronic acid pinacol ester (15 µmol), copper(II) triflate (5 µmol), and pyridine (25 µmol), in DMA (700 µl) was then carried out at 120 °C for 20 minutes under an atmosphere of air (Scheme 1). Each reaction was quenched with 0.2 M HCl (1 ml) to ensure the dissolution of all [^{18}F]fluoride from the reaction vessel walls. The radiochemical yield (%RCY) was evaluated using radioTLC to measure reaction performance, and selected experiments were evaluated with radioHLPC to confirm compound identity.

Using standard published QMA processing methods (Table 1, entries 1 and 2) yielded good recoveries of [^{18}F]fluoride; however, as expected, the model CMRF reactions did not tolerate the presence of Kryptofix and potassium carbonate. The elimination of Kryptofix using conditions similar to those published by Makaravage *et al.* (and those used in our previous work) improved CMRF reaction performance (Table 1, entries 3 and 4). These experiments also demonstrated the importance of the QMA cartridge preconditioning anion, as reaction performance again increased when the QMA cartridges were conditioned with potassium triflate (0.5 M, 10 ml) instead of sodium bicarbonate (1 M, 10 ml).

Entries 5–7 showed that TBAOTf in water possessed sufficient eluting power to quantitatively recover [^{18}F]fluoride from the QMA cartridge without the need for an additional carbonate base. We then attempted to elute the ^{18}F with methanol *via* a protocol similar to that of the minimalist approach employed by Zischler and coworkers (Table 1, entries 8 and 9). The ^{18}F was loaded onto the QMA cartridge in the reverse direction (back-flushing) and then washed with methanol in the forward direction to remove any residual water, after which the ^{18}F could be recovered by eluting with TBAOTf in methanol (1 ml, 5–10 mg ml^{-1}). However, much of the ^{18}F was lost during the methanol wash step. This was possibly due to a combination of the ^{18}F being loaded on the front end of the cartridge and the use of a triflate QMA counterion over the standard bicarbonate ion used in previous works.

We then attempted an alternative procedure, loading the ^{18}F onto the QMA cartridge in the forward direction, followed by washing with methanol and eluting the ^{18}F with the same TBAOTf solution as before (Table 1, entry 15). To our delight, this afforded [^{18}F]TBAF in methanol with acceptable relative ^{18}F recoveries (93 ± 2.2%). The methanol could then be removed *via* evaporation at 85 °C under a stream of argon to afford dry and carbonate-free [^{18}F]TBAF. The model CMRF

reaction showed excellent reaction performance with both single batch and aliquoted [^{18}F]TBAF prepared in this manner. Additionally, the reaction showed tolerance to TBAOTf loads between 5–10 mg (Table 1, entries 14 and 15). Lower TBAOTf loads (1 mg) in the QMA eluent solution often failed to completely elute the ^{18}F from the QMA cartridge and negatively influenced reaction performance (Table 1, entry 16). Finally, we evaluated the importance of the methanol wash step to remove residual water from the QMA cartridge (Table 1, entry 17). Skipping this step resulting in marginally higher % ^{18}F recoveries and, unexpectedly, had no significantly deleterious effects on reaction performance. Furthermore, the elimination of the methanol wash increased the method's operational simplicity so that it can be used directly on most ^{18}F automated synthesizers, a further advantage when considering prospective large-scale routine radiotracer productions.

We also evaluated both acetonitrile and ethanol as alternative elution solvents, with ethanol being more suited to clinical radiotracer production due to its lower toxicity compared to acetonitrile or methanol (Table 1, entries 10–13). TBAOTf in acetonitrile was unable to elute any ^{18}F from the QMA, suggesting that protic solvents are required for this method to work. TBAOTf in ethanol successfully eluted the ^{18}F, albeit with slightly weaker elution efficiency and lower reaction performance.

To evaluate our ^{18}F processing method's performance and scalability, we applied it to a DoE optimization and subsequent radiosynthesis automation of [^{18}F]olaparib. [^{18}F]Olaparib is a tracer of potential clinical importance as a "second-generation" variant of [^{18}F]PARPi, a radiotracer that is currently in clinical trials for the imaging of the DNA repair enzyme PARP-1.[25,26] The recently reported copper-mediated radiosynthesis of [^{18}F]olaparib reacts azeotropically dried [^{18}F]KF (eluted from a QMA cartridge using Kryptofix, potassium carbonate, and potassium oxalate (Table 1, entry 1)) with a trimethylsilylethoxymethyl (SEM) protected pinacol boronate precursor **OLA-BPin**, in the presence of [Cu(OTf)$_2$(Impy)$_4$] as the copper mediator (Scheme 2).[27] The reaction is carried out under air in 1,3-dimethyl-2-imidazolidinone (DMI) at 120 °C for 20 minutes, after which the SEM protecting group is removed by stirring the reaction mixture with TFA at 120 °C for a further 15 minutes to afford [^{18}F]olaparib after HPLC purification (activity yield: 6 ± 5%, automated process).[25,27]

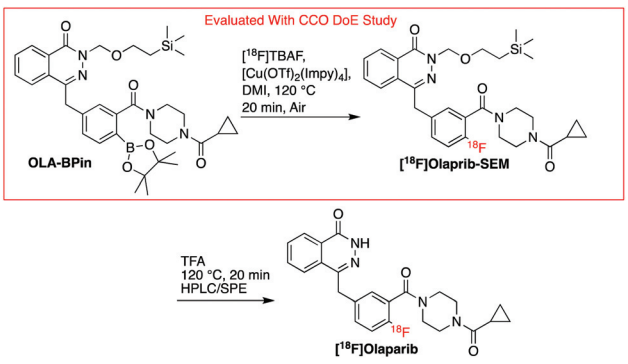

Scheme 2 Radiosynthesis of [^{18}F]olaparib *via* the CMRF of the precursor OLA-BPin.

Having synthesized the arylboronate precursor *via* the published route (see ESI 1.2†), we used the DoE software MODDE Go (Sartorious, Germany) to design a response surface optimization study of the CMRF step using an orthogonal central composite design (CCO) (see ESI 3.2.4†). The resulting study consisted of 17 experiments (14 experimental points, 3 centerpoints) to evaluate the effects of the precursor load (Pre, 5–25 μmol), copper mediator load (CuC, 5–25 μmol), and solvent volume (SoV, 300–600 μl) on the reaction's performance (ESI Table 1†). The DoE study was conducted using three ^{18}F cyclotron target washes (over three days), each trapped and eluted from a single QMA cartridge. The resulting methanolic [^{18}F]TBAF solution was then aliquoted (150 μl) into single-use glass reaction tubes (6 runs per target wash), and the methanol was evaporated from each reaction vessel at 90 °C under a stream of argon. Finally, the reaction mixture required by the DoE study was added to the dry [^{18}F]TBAF, and the reaction was allowed to stir for 120 °C for 20 minutes. After quenching with 0.1 M HCl, the reaction performance (%RCY) of the CMRF step was measured by radioTLC, and selected runs were analyzed *via* radioHPLC to verify product identity against a non-radioactive standard.

After acquiring the %RCY data, the resulting data set was found to be skewed and was thus transformed ($-\log_{10}Y$) to ensure a normal distribution. Multiple linear regression (MLR) was used to construct a response surface model from the transformed data set; the summary of fit statistics suggested the resulting model to be valid and predictive (R^2 = 0.972 (goodness of model fit); Q^2 = 0.900 (goodness of model prediction); ESI Fig. 5)†. The results of the DoE study showed all main factors (precursor load, copper mediator load, and solvent volume) to have significant effects %RCY (ESI Fig. 6†). The copper mediator load, precursor load, and solvent volume terms were found to possess significant quadratic behaviors (they contribute to curvature in the response surface). Moreover, factor interactions (where one setting affects the behavior of another) between the precursor and copper mediator loads and between the copper mediator load and the solvent volume (copper mediator concentration) were detected. Plotting the response surface over the investigated ranges revealed that the CMRF synthesis of [^{18}F]olaparib performed better at lower reaction concentrations (higher solvent volume) and that the optimal amounts of the precursor and copper mediator were approximately 10 μmol and 22 μmol, respectively (Fig. 2).

To verify the DoE study results and the scalability of the ^{18}F processing method, the radiolabeling of [^{18}F]olaparib was performed manually in triplicate using two sets of optimal conditions from the response surface model. A full batch preparation of [^{18}F]TBAF was used for each replicate experiment instead of aliquots of [^{18}F]TBAF from a single QMA cartridge elution. Performing the synthesis with 10.5 μmol **OLA-BPin** (7 mg), 22 μmol [Cu(OTf)$_2$(Impy)$_4$] (18 mg), and 600 μl DMI (total solvent volume) afforded the SEM protected radiolabeled intermediate [^{18}F]olaparib-SEM in good radiochemical yields

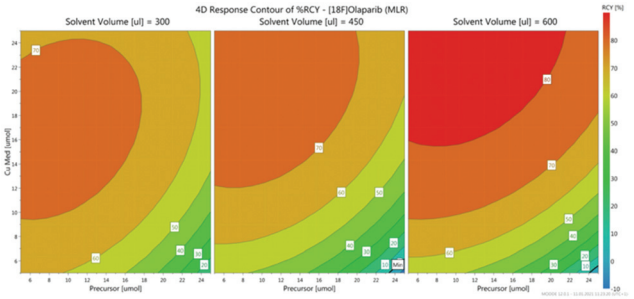

Fig. 2 4D-plot of the response surface model generated from the DoE optimization study of the CMRF synthesis of [^{18}F] olaparib.

in line with those predicted by the response surface model (78 ± 6%RCY, n = 4, DoE Response surface predicted 84%, ESI Fig. 13: Validation Set A).† The validity of the model was again tested by performing the same synthesis using 15.6 μmol **OLA-BPin** (10.5 mg) and 26 μmol [Cu(OTf)$_2$(Impy)$_4$] (22 mg), in 600 μl DMI. These conditions again afforded [^{18}F]olaparib-SEM in good radiochemical yields (85 ± 3%RCY, n = 3, DoE Response surface predicted 83%, ESI Fig. 13: Validation Set B).† These conditions proved slightly better but used more of the expensive copper-mediator and precursor; therefore, the previous conditions were favored for further development. Beyond these "optimal" validation experiments, we performed a series of "batch" experiments that aimed to test the validity of the model under non-optimal reaction conditions (ESI Fig. 13: Alternative Set).† Overall, there seems to be a reasonable correlation (r = 0.9386) between the results obtained in validation experiments conducted with batches of [^{18}F]TBAF and the results predicted by the DoE study (generated with aliquots of [^{18}F]TBAF.)

Deprotection with TFA (700 μl) at 120 °C for 15 minutes was found to remove the SEM protecting group with >95% efficiency to afford [^{18}F]olaparib.

The optimized [^{18}F]olaparib radiosynthesis was translated onto both a Tracerlab FX N Pro (GE, Uppsala, Sweden) and an Elixys FLEX/CHEM radiosynthesizer to measure the total radiosynthesis performance (activity yield, %AY) and to prepare the tracer for preclinical imaging experiments (see ESI 3.3†). The synthesis was performed *via* a modified version of the process described in the literature.[27] When performed using an Elixys FLEX/CHEM coupled to a PURE/FORM synthesis module (Sofie Bioscience, USA), the optimized synthesis was able to afford [^{18}F]olaparib with a non-decay corrected activity yield (%AY) up to 41% (80% RCY (decay corrected), 25–58 GBq μmol^{-1}, (ESI Table 3)),† a significant improvement over the synthesis described by Guibbal *et al.*[27]

The performance of the synthesis using an FX N Pro was initially found to be significantly lower than expected (5.4 ± 1.6%AY; 9.3 ± 3.3%RCY, n = 4, ESI Table 5).† However, sampling of the reaction product mixture before deprotection and purification revealed the CMRF step to perform within the range predicted by the response surface (59%RCY, n = 1). This strongly suggests that a large percentage of the product radioactivity is lost elsewhere in the process when using the FX N Pro. Further investigation found that this most likely occurs during the first HLB trapping of the product before HPLC purification. The FX N pro is limited to a dilution volume of *ca.* 14 ml, while a larger dilution reservoir (25–100 ml) can be fitted between cassettes one and two of the Elixys. The larger dilution volume makes Elixys HLB "pre-purification" more efficient, resulting in an overall %RCY that is more in line with the results predicted by the DoE response surface. More work is thus needed to improve the overall process performance on the FX N Pro. These results highlight that the optimization of a radiochemical process is as important as the optimization of the radiochemistry. However, detailed DoE optimization of the radiolabeling chemistry can provide a greater margin of error when designing automated radiosynthetic processes.

Conclusions

In conclusion, we have implemented an ^{18}F processing method that is compatible with CMRF reaction conditions on both small (experiments using aliquots of QMA eluted [^{18}F]TBAF) and large scale (single batch) radiosyntheses. Moreover, through the synthesis of [^{18}F]olaparib, we could demonstrate that [^{18}F]TBAF produced in this way can be conveniently used for small scale CMRF optimization studies using DoE, and importantly, that these results can then be scaled up to full batch tracer productions which can be performed using automated radiosynthesizers. We have shown that this ^{18}F processing method can unlock the potential of the DoE approach to aid in the establishment of efficient radiotracer production processes using the CMRF methodology. This will further expedite both the preclinical tracer development process and the translation of the CMRF methodology to routine clinical tracer productions.

Author contributions

Gregory Bowden (G.B.) and Nantanat Chailangger designed and performed the radiochemical experiments. G.B. performed the organic synthesis and chemically characterized the compounds. G.B. designed the DoE study and analyzed the data. G.B. established the automated radiosyntheses on both the Elixys FLEX/CHEM and GE FX N Pro. The manuscript was written and reviewed by G.B., Andreas Maurer, and Bernd Pichler.

Conflicts of interest

There are no conflicts to declare.

Acknowledgements

We would like to thank the Adolf Leuze Foundation and the Werner Siemens Stiftung for their financial contributions

toward this work. Funding for this work was also provided by the Deutsche Forschungsgemeinschaft (DFG, German Research Foundation) under Germany's Excellence Strategy – EXC 2180–390900677. We would also like to thank Dr Gerald Reischl, Marko Matijevic, and other colleagues in the radiopharmacy at the Werner Siemens Imaging Center for the delivery of [^{18}F]fluoride and for technical support.

Notes and references

1 M. Tredwell, S. M. Preshlock, N. J. Taylor, S. Gruber, M. Huiban, J. Passchier, J. Mercier, C. Génicot and V. Gouverneur, *Angew. Chem., Int. Ed.*, 2014, **53**, 7751–7755.
2 A. V. Mossine, A. F. Brooks, K. J. Makaravage, J. M. Miller, N. Ichiishi, M. S. Sanford and P. J. H. Scott, *Org. Lett.*, 2015, **17**, 5780–5783.
3 K. J. Makaravage, A. F. Brooks, A. V. Mossine, M. S. Sanford and P. J. H. Scott, *Org. Lett.*, 2016, **18**, 5440–5443.
4 J. S. Wright, T. Kaur, S. Preshlock, S. S. Tanzey, W. P. Winton, L. S. Sharninghausen, N. Wiesner, A. F. Brooks, M. S. Sanford and P. J. H. Scott, *Clin. Transl. Imaging*, 2020, **8**, 167–206.
5 L. Allott and E. O. Aboagye, *Mol. Pharm.*, 2020, **17**, 2245–2259.
6 P. M. Murray, F. Bellany, L. Benhamou, D.-K. Bučar, A. B. Tabor and T. D. Sheppard, *Org. Biomol. Chem.*, 2016, **14**, 2373–2384.
7 G. D. Bowden, B. J. Pichler and A. Maurer, *Sci. Rep.*, 2019, **9**, 11370.
8 B. D. Zlatopolskiy, J. Zischler, P. Krapf, F. Zarrad, E. A. Urusova, E. Kordys, H. Endepols and B. Neumaier, *Chem. – Eur. J.*, 2015, **21**, 5972–5979.
9 S. Preshlock, S. Calderwood, S. Verhoog, M. Tredwell, M. Huiban, A. Hienzsch, S. Gruber, T. C. Wilson, N. J. Taylor, T. Cailly, M. Schedler, T. L. Collier, J. Passchier, R. Smits, J. Mollitor, A. Hoepping, M. Mueller, C. Genicot, J. Mercier and V. Gouverneur, *Chem. Commun.*, 2016, **52**, 8361–8364.
10 A. V. Mossine, A. F. Brooks, N. Ichiishi, K. J. Makaravage, M. S. Sanford and P. J. H. Scott, *Sci. Rep.*, 2017, **7**, 233.
11 S. O. Lahdenpohja, N. A. Rajala, J. Rajander and A. K. Kirjavainen, *EJNMMI Radiopharm. Chem.*, 2019, **4**, 28.
12 X. Zhang, F. Basuli and R. E. Swenson, *J. Labelled Compd. Radiopharm.*, 2019, **62**, 139–145.
13 D. Antuganov, M. Zykov, V. Timofeev, K. Timofeeva, Y. Antuganova, V. Orlovskaya, O. Fedorova and R. Krasikova, *Eur. J. Org. Chem.*, 2019, **2019**, 918–922.
14 R. Richarz, P. Krapf, F. Zarrad, E. A. Urusova, B. Neumaier and B. D. Zlatopolskiy, *Org. Biomol. Chem.*, 2014, **12**, 8094–8099.
15 F. Zarrad, B. Zlatopolskiy, P. Krapf, J. Zischler and B. Neumaier, *Molecules*, 2017, **22**, 2231.
16 J. Zischler, N. Kolks, D. Modemann, B. Neumaier and B. D. Zlatopolskiy, *Chem. – Eur. J.*, 2017, **23**, 3251–3256.
17 J. A. H. Inkster, V. Akurathi, A. W. Sromek, Y. Chen, J. L. Neumeyer and A. B. Packard, *Sci. Rep.*, 2020, **10**, 6818.
18 K. Bratteby, V. Shalgunov, U. Battisti, I. Petersen, S. Broek, T. Ohlsson, N. Gillings, M. Erlandsson and M. Herth, 2021, ChemRxiv, This content is a preprint and has not been peer-reviewed.
19 M. T. Morales-Colón, Y. Y. See, S. J. Lee, P. J. H. Scott, D. C. Bland and M. S. Sanford, *Org. Lett.*, 2021, **23**, 4493–4498.
20 K. M. Engle, L. Pfeifer, G. W. Pidgeon, G. T. Giuffredi, A. L. Thompson, R. S. Paton, J. M. Brown and V. Gouverneur, *Chem. Sci.*, 2015, **6**, 5293–5302.
21 W. K. Dong, H. J. Jeong, T. L. Seok, M. H. Sohn, J. A. Katzenellenbogen and Y. C. Dae, *J. Org. Chem.*, 2008, **73**, 957–962.
22 D. W. Kim, H. J. Jeong, S. T. Lim and M. H. Sohn, *Angew. Chem., Int. Ed.*, 2008, **47**, 8404–8406.
23 V. Orlovskaya, D. Antuganov, O. Fedorova, V. Timofeev and R. Krasikova, *Appl. Radiat. Isot.*, 2020, **163**, 109195.
24 R. N. Krasikova, *Molecules*, 2020, **25**, 4365.
25 T. C. Wilson, M.-A. Xavier, J. Knight, S. Verhoog, J. B. Torres, M. Mosley, S. L. Hopkins, S. Wallington, P. D. Allen, V. Kersemans, R. Hueting, S. Smart, V. Gouverneur and B. Cornelissen, *J. Nucl. Med.*, 2019, **60**, 504–510.
26 B. Carney, G. Carlucci, B. Salinas, V. Di Gialleonardo, S. Kossatz, A. Vansteene, V. A. Longo, A. Bolaender, G. Chiosis, K. R. Keshari, W. A. Weber and T. Reiner, *Mol. Imaging Biol.*, 2016, **18**, 386–392.
27 F. Guibbal, P. G. Isenegger, T. C. Wilson, A. Pacelli, D. Mahaut, J. B. I. Sap, N. J. Taylor, S. Verhoog, S. Preshlock, R. Hueting, B. Cornelissen and V. Gouverneur, *Nat. Protoc.*, 2020, **15**, 1525–1541.

